Is There a Transition-State Imbalance for Proton Transfers in the Gas Phase? *Ab Initio* Study of the Carbon-to-Carbon Proton Transfer from Acetaldehyde to Its Enolate Ion

Claude F. Bernasconi* and Philip J. Wenzel

Contribution from the Department of Chemistry and Biochemistry, University of California, Santa Cruz, California 95064

Received December 10, 1993. Revised Manuscript Received March 22, 1994®

Abstract: The identity proton transfer between acetaldehyde and its enolate ion has been studied by *ab initio* methods. Two transition states, a "cis-gauche" and a "trans-anti", have been calculated. Both transition states are characterized by a charge imbalance in the sense that charge delocalization into the carbonyl group of the incipient *product* enolate ion lags behind proton transfer or charge localization on the α-carbon of the *reactant* enolate ion is ahead of proton transfer. The imbalance for the cis-gauche TS, which is a fully optimized structure, is larger than that for the trans-anti TS. This is a consequence of only partially optimizing the structure of the trans-anti TS by constraining the α-carbon to a planar geometry; hence, the trans-anti TS represents a model for a more delocalized transition state. At the MP2/6-311+G** level, the cis-gauche TS is 10.5 kcal/mol lower in energy than the trans-anti TS. Possible reasons why the less delocalized and more imbalanced cis-gauche TS is more stable than the more delocalized trans-anti TS are discussed. The reaction paths implied by the imbalanced transition states are conveniently described by means of 6-corner, hexagonal More O'Ferrall–Jencks diagrams. Corners 1 and 4 define the reactants and products, respectively; corners 2 and 3, which are 13 kcal/mol above the reactants/products, represent a hypothetical intermediate with the geometry of the acetaldehyde with the negative charge localized on the α-carbon ("aldanion"); and corners 5 and 6, which are 25.4 kcal/mol above the reactants/products, are approximated by the polarized structure $H^+CH_2{=}CH{-}O^-$ with the geometry of the enolate ion ("enaldehyde"). The trans-anti TS also shows a *structural* imbalance in the sense that C—C π-bond formation in the incipient product enolate ion is somewhat ahead of proton transfer; no such imbalance is found for the cis-gauche TS.

Introduction

Proton transfers are among the most important elementary processes in chemistry and consequently have received much attention. The main focus has been on proton transfers in solution, which have been reviewed frequently.[1-10] More recently there has been a growing interest in the study of these reactions in the gas phase[11-19] and also in quantum mechanical calculations.[20-28]

The present paper describes an *ab initio* study of the carbon-to-carbon proton transfer from acetaldehyde to its enolate ion, eq 1. A major question we would like to address is to what extent

$$O{=}CH{-}CH_3 + CH_2{=}CH{-}O^- \rightleftharpoons {}^-O{-}CH{=}CH_2 + CH_3{-}CH{=}O \quad (1)$$

the transition-state imbalances commonly observed in proton transfers from carbon acids in solution also occur in the gas phase. The term imbalance is generally used to describe a situation where various processes such as bond formation/bond cleavage, development or destruction of charge and π-overlap (resonance), solvation/desolvation, etc. have made unequal progress or have developed nonsynchronously at the transition state.[10,29]

* Abstract published in *Advance ACS Abstracts*, May 1, 1994.

(1) Eigen, M. *Angew. Chem., Int. Ed. Engl.* **1964**, *3*, 1.
(2) Ritchie, C. D. In *Solute–Solvent Interactions*; Coetzee, J. F., Ritchie, C. D., Eds.; Dekker: New York, 1969; Chapter 4.
(3) (a) Kresge, A. *J. Chem. Soc. Rev.* **1973**, *2*, 475. (b) Kresge, A. *J. Acc. Chem. Res.* **1975**, *8*, 354.
(4) Bell, R. P. *The Proton in Chemistry*, 2nd ed.; Cornell University Press; Ithaca, NY, 1973; Chapter 10.
(5) Jones, J. R. *The Ionization of Carbon Acids*; Academic Press: New York, 1973.
(6) Caldin, E. F.; Gold, V., Eds. *Proton Transfer Reactions*; Wiley & Sons: New York, 1975.
(7) Hibbert, F. *Compr. Chem. Kinet.* **1977**, *8*, 97.
(8) Koch, H. F. *Acc. Chem. Res.* **1984**, *17*, 137.
(9) Stewart, R. *The Proton: Applications to Organic Chemistry*; Academic Press: New York, 1985.
(10) Bernasconi, C. F. *Adv. Phys. Org. Chem.* **1992**, *27*, 116.
(11) (a) Farneth, W. E.; Brauman, J. I. *J. Am. Chem. Soc.* **1976**, *98*, 7891. (b) Moylan, C. R.; Brauman, J. I. *Annu. Rev. Phys. Chem.* **1983**, *34*, 187. (c) Moylan, C. R.; Jasinski, J. M.; Brauman, J. I. *J. Am. Chem. Soc.* **1985**, *107*, 1934. (d) Han, C.-C.; Dodd, J. A.; Brauman, J. I. *J. Phys. Chem.* **1986**, *90*, 471. (e) Dodd, J. A.; Baer, S.; Moylan, C. R.; Brauman, J. I. *J. Am. Chem. Soc.* **1991**, *113*, 5942.
(12) Bowers, M. T., Ed. *Gas Phase in Chemistry*; Academic Press: New York, 1979.
(13) Ausloos, P.; Lias, S. G. *J. Am. Chem. Soc.* **1981**, *103*, 3641.
(14) (a) Mackay, G. I.; Bohme, D. K. *Int. J. Mass Spectrom. Ion Phys.* **1978**, *26*, 327. (b) Bohme, D. K.; Rakshit, A. B.; Mackay, G. I. *J. Am. Chem. Soc.* **1982**, *104*, 1100.
(15) (a) Larson, J. W.; MacMahon, T. B. *J. Phys. Chem.* **1987**, *91*, 554. (b) Fuke, K.; Yabe, T.; Chiba, N.; Kohida, T.; Kaya, K. *Ibid.* **1986**, *90*, 2309.
(16) Hierl, P. M.; Ahrens, A. F.; Henchman, M.; Viggiano, A. A.; Paulson, J. F. *J. Am. Chem. Soc.* **1986**, *108*, 3140.
(17) Brickhouse, M. D.; Squires, R. R. *J. Am. Chem. Soc.* **1988**, *110*, 2706.
(18) Ikonomou, M. G.; Sunner, J.; Kebarle, P. *J. Phys. Chem.* **1988**, *92*, 6308.
(19) Meot-Ner (Mautner), M.; Smith, S. C. *J. Am. Chem. Soc.* **1991**, *113*, 862.
(20) (a) Scheiner, S. *Acc. Chem. Res.* **1985**, *18*, 174. (b) Latajka, Z.; Scheiner, S. *Int. J. Quantum Chem.* **1986**, *29*, 285. (c) Cybulski, S. M.; Scheiner, S. *J. Am. Chem. Soc.* **1987**, *109*, 4199. (d) Cybulski, S. M.; Scheiner, S. *Ibid.* **1989**, *111*, 23. (e) Scheiner, S.; Wang, L. *Ibid.* **1992**, *114*, 3640. (f) Duan, X.; Scheiner, S. *Ibid.* **1992**, *114*, 5849. (g) Latajka, Z.; Scheiner, S. *J. Phys. Chem.* **1992**, *96*, 9764. (h) Isaacson, A. D.; Wang, L.; Scheiner, S. *Ibid.* **1993**, *97*, 1765.
(21) Cao, H. Z.; Allaverra, M.; Tapia, O.; Evleth, E. M. *J. Phys. Chem.* **1985**, *89*, 1581.
(22) Cukier, R. I.; Morillo, M. *J. Chem. Phys.* **1989**, *91*, 857.
(23) McKee, M. L. *J. Am. Chem. Soc.* **1987**, *109*, 559.
(24) (a) Bosch, E.; Lluch, J. M.; Bertran, J. *J. Am. Chem. Soc.* **1990**, *112*, 3868. (b) Bosch, E.; Moreno, M.; Lluch, J. M. *Can. J. Chem.* **1992**, *70*, 100.
(25) Wolfe, S.; Hoz, S.; Kim, C.-K.; Yang, K. *J. Am. Chem. Soc.* **1990**, *112*, 4186.
(26) Truong, T. N.; McCammon, J. A. *J. Am. Chem. Soc.* **1991**, *113*, 7504.
(27) Saunders, W. H., Jr. *J. Am. Chem. Soc.*, preceding paper in this issue.
(28) Gronert, S. *J. Am. Chem. Soc.* **1993**, *115*, 10258.
(29) (a) Jencks, D. A.; Jencks, W. P. *J. Am. Chem. Soc.* **1977**, *99*, 7948. (b) Jencks, W. P. *Chem. Rev.* **1985**, *85*, 511.

0002-7863/94/1516-5405$04.50/0

Imbalances are often recognized on the basis of structure–reactivity coefficients when substituents at different positions of the transition state give conflicting reports about charge development at the reaction site. One of the best known examples is the deprotonation of arylnitroalkanes by amines or hydroxide ion (eq 2), where the Brønsted α_{CH} value (1.29) determined by varying

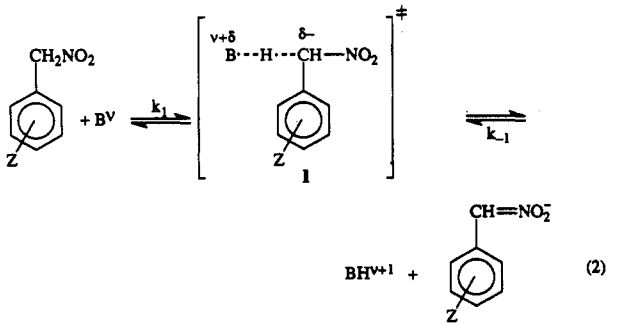

(2)

the Z substituent is much larger than the Brønsted β_B value (0.56) obtained by varying the substituent in B^v.[30] The generally accepted interpretation for $\alpha_{CH} > \beta_B$ is that delocalization of the negative charge into the nitro group lags behind proton transfer, i.e., at the transition state the central carbon is still largely sp^3-hybridized and bears most of the negative charge.[31]

This situation can schematically be illustrated by means of the More O'Ferrall[32]–Jencks[29,33] diagram of Figure 1. The lower left corner represents the reactants and the upper right corner the products, while the lower right corner is a hypothetical intermediate whose negative charge is completely localized on the sp^3-hybridized carbon. The hypothetical intermediate in the upper left corner is less clearly defined but is probably best represented by a structure that indicates a polarization akin to that implied by hyperconjugation.[34] The progress variables on the diagram are thus the degree of proton transfer (horizontal axes) and the degree of charge delocalization into the nitro group (vertical axes); in solution the solvation of the nitro group is undoubtedly included in the vertical axes.[31,36] A synchronous development of the two progress variables would correspond to the diagonal reaction coordinate, while the actual reaction coordinate, corresponding to the observed imbalance, is shown by the curved line. The location of the transition state in the lower right half of the diagram is not only imposed by the observed lag in the charge delocalization behind proton transfer (most easily seen from the projections of the reaction coordinate onto the two axes) but also implied by the higher energy of the upper left corner relative to the lower right corner of the diagram.[36]

It should be noted that Bordwell and Boyle[30] considered the carbanion in the lower right corner of Figure 1 to be an *actual* intermediate, stabilized by hydrogen-bonding solvation of the charge by water. This implies that the reaction is stepwise, the first step being rate-limiting and occurring along the lower horizontal axis, and the second step corresponding to the right vertical axis of the diagram. There is little experimental support

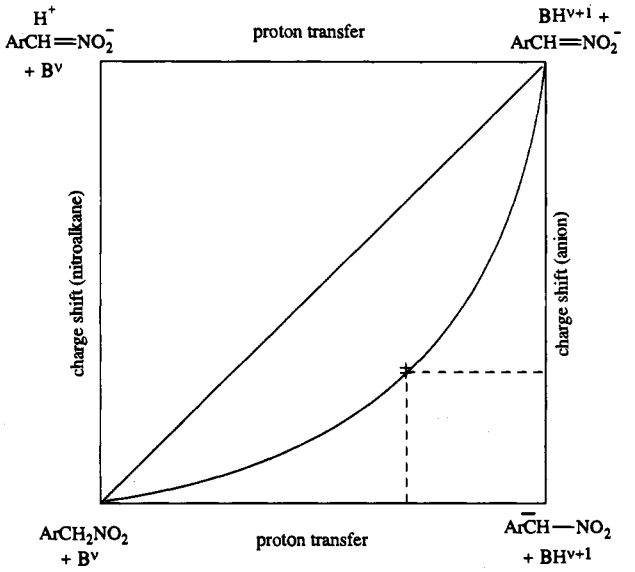

Figure 1. More O'Ferrall–Jencks diagram with separate axes for proton transfer and charge shifts, illustrating the lag in charge shift behind proton transfer in the deprotonation of arylnitroalkanes by OH^- or amines.

for this extreme view, though, and a kinetic carbon isotope effect study[37] essentially rules it out.

The lack of synchronization between proton transfer and charge delocalization appears to be a general phenomenon in the deprotonation of carbon acids activated by π-acceptors.[31] The question *why* such imbalances occur is of considerable interest. A consequence of the lag in charge delocalization is that there is little development of resonance stabilization of the transition state, which is a major reason why reactions that lead to resonance-stabilized products have high intrinsic barriers.[31] This state of affairs seems to contradict a basic law of nature, according to which physical or chemical processes should always follow a path of minimum energy. The apparent contradiction is that the lag in resonance development seems to create a higher barrier than would prevail if this resonance development were synchronous with proton or charge transfer. Thus, one wonders why resonance does not develop synchronously with proton or charge transfer.

An appealing qualitative explanation as to why charge imbalances occur has been offered by Kresge[38] and can be illustrated by the generalized reaction scheme of eq 3, in which Y represents a π-acceptor group. According to Kresge, the degree

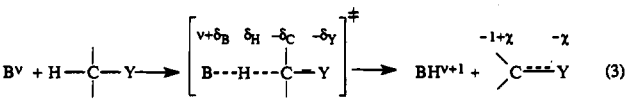

(3)

of charge delocalization into Y should be intimately related to the degree of C–Y double bond formation, which in turn depends on the fraction of charge that has been transferred from the base to the substrate. Hence the charge on Y at the transition state will be quite small since it is a fraction of a fraction. Another factor that may reduce the delocalization into Y at the transition state is electrostatic attraction between the transferred proton and the charge on the α-carbon,[38] especially if the transferred proton carries a partial positive charge (δ_H).

In a recent attempt[10,39] at quantifying Kresge's model, the following assumptions were made. (1) At the transition state, the total negative charge on the >C–Y moiety ($\delta_C + \delta_Y$ in eq 3) is distributed between C and Y in such a way that the charge on Y (δ_Y) is equal to the total charge on the >C–Y moiety

(30) Bordwell, F. G.; Boyle, W. J., Jr. *J. Am. Chem. Soc.* **1972**, *94*, 3907; **1975**, *97*, 3447.
(31) For reviews, see: (a) Bernasconi, C. F. *Tetrahedron* **1985**, *41*, 3234. (b) Bernasconi, C. F. *Acc. Chem. Res.* **1987**, *20*, 301. (c) Reference 10.
(32) More O'Ferrall, R. A. *J. Chem. Soc. B* **1970**, 274.
(33) Jencks, W. P. *Chem. Rev.* **1972**, *72*, 705.
(34) An alternative representation is to leave the upper left corner undefined and assume that, because of its high energy, its influence on the reaction is minimal.[35]
(35) Jencks and Jencks[29] have described the reaction with a three-corner diagram, omitting the upper left corner altogether.
(36) Albery, W. J.; Bernasconi, C. F.; Kresge, A. J. *J. Phys. Org. Chem.* **1988**, *1*, 29.
(37) Wilson, J. C.; Källsson, I.; Saunders, W. H., Jr. *J. Am. Chem. Soc.* **1980**, *102*, 4780.
(38) Kresge, A. J. *Can. J. Chem.* **1974**, *52*, 1897.
(39) Bernasconi, C. F. *Acc. Chem. Res.* **1992**, *25*, 9.

multiplied by the π-bond order of the C–Y bond, eq 4. (2) The

$$\delta_Y = \pi_{bo}(\delta_C + \delta_Y) \quad (4)$$

$$\pi_{bo} = \chi(\delta_C + \delta_Y) \quad (5)$$

$$\delta_Y = \chi(\delta_C + \delta_Y)^n \quad (6)$$

π-bond order, in turn, is proportional to the total charge $\delta_C + \delta_Y$, eq 5, with the proportionality constant, χ, being equal to the charge on Y in the *product ion*. This leads to eq 6 with $n = 2$. As a further simplification, it was assumed that $\delta_H = 0$, which reduces $\delta_C + \delta_Y$ to δ_B and $\delta_C = \delta_B - \delta_Y = \delta_B - \chi(\delta_B)^n$.

Using reaction 2 for illustration and equating $\delta_C + \delta_Y = \delta_B$ with the experimental Brønsted β_B value of 0.56,[30] one obtains $\delta_Y = 0.314\chi$ and $\delta_C = 0.246\chi$. Since the nitro group is such a strong π-acceptor, χ is likely to be close to unity,[38] in which case $\delta_Y \approx 0.314$ and $\delta_C \approx 0.246$. For a reaction with a weaker π-acceptor, e.g., with $\chi = 0.5$, one would obtain $\delta_Y = 0.157$ and $\delta_C = 0.403$ assuming $\delta_B = 0.56$.

As pointed out by Kresge,[38] direct proportionality between delocalization and π-bond order or between π-bond order and δ_B not necessarily apply, though, in which case n may be >2 or <2.[40] Note, however, that imbalance requires that $n > 1$. This is because, by definition, imbalance implies that the ratio of the charge on Y to the charge on C is smaller at the transition state than in the product ion, i.e., $\delta_Y/\delta_C < \chi/(1 - \chi)$. This is only possible if $n > 1$. By the same token, $n < 1$ would mean an imbalance in the sense that charge delocalization is ahead of proton transfer, i.e., $\delta_Y/\delta_C > \chi/(1 - \chi)$, while $n = 1$ means that delocalization is synchronous with proton transfer, i.e., $\delta_Y/\delta_C = \chi/(1 - \chi)$. Application of eq 4 to a number of proton transfers in aqueous and other solvents suggests an approximate value of n between 2 and 3.[10]

The imbalanced transition state in the deprotonation of nitroalkanes has also been discussed in the context of the valence bond configuration mixing model developed by Shaik and Pross.[41] In their terminology, the product configuration (negative charge on oxygen) is a diexcited configuration which is of high energy in the early phases of the reaction. In contrast, the intermediate configuration (negative charge on carbon) is monoexcited and of lesser energy in the early phases of the reaction. Hence the intermediate configuration makes a larger contribution to the transition state than the product configuration. In the late phases of the reaction coordinate, the relative energies of intermediate and product configurations are reversed, and the product configuration becomes dominant.

An important but unresolved question is how much of the transition state imbalances may be attributed to solvation effects, e.g., to a lag in the solvation of the charge on the Y group in eq 3.[10,42,43] This question is difficult to answer experimentally, but *ab initio* calculations of transition-state structures offer a viable approach. Acetaldehyde was chosen for the present study because it is one of the simplest carbon acids activated by a π-acceptor group. The choice of the enolate ion as base offers the advantage of a reaction with a symmetrical transition state which facilitates the interpretation of the results. Our calculations suggest that eq 1 exhibits a transition state that is nearly tetrahedral with respect to the geometry of the acidic carbon atom. Such an imbalanced transition state, in which electronic reorganization (charge delocalization into the carbonyl group) lags behind proton transfer, is in qualitative agreement with the kind of imbalances observed in solution proton transfers. Our calculations have also located a "constrained" transition state with nearly planar geometry of the acidic carbon, in which electronic reorganization is more synchronous with proton transfer. Interestingly, this more balanced transition state is of higher energy than the strongly imbalanced one.

Table 1. Energies of Reactants, Hypothetical Intermediates, and Transition States (6-311+G**)

	SCF (hartree)	MP2 (hartree)	ZPE[a] (kcal/mol)
aldehyde(e)	−152.961 580	−153.448 080	36.03
aldehyde(s)	−152.960 799	−153.446 789	35.92
enolate ion	−152.350 918	−152.849 192	28.38
"enaldehyde"	−152.910 165	−153.406 425	36.29
"aldanion"	−152.329 630	−152.827 768	28.15
cis-gauche TS	−305.286 484	−306.295 627	64.37
trans-anti TS	−305.266 536	−306.279 415	64.72
cis-gauche TS-H$^+$ [b]	−304.539 271	−305.553 321	55.50
trans-anti TS-H$^+$ [b]	−304.563 584	−305.570 474	56.91

[a] At 298 K, scaled above 500 cm^{-1}. [b] Energy of transition state after removal of the acidic proton.

Table 2. Ionization Energies, Rearrangement Energies, and Reaction Barriers[a]

	ΔE		ΔH[b]	
	SCF	MP2	SCF	MP2
aldehyde(e) → enolate ion	383.20	375.80	375.55	368.15[d]
aldehyde(s) → enolate ion	382.70	374.99	375.16	367.45
aldehyde(e) → "enaldehyde"	32.26	26.14	32.52	25.40
aldehyde(s) → "enaldehyde"	31.77	25.33	32.14	25.70
enolate ion → "aldanion"	13.13	13.21	12.90	12.98
reactants(e) → cis-gauche TS	16.32	1.04	16.28	1.00
reactants(s) → cis-gauche TS	15.83	0.22	15.90	0.29
reactants(e) → trans-anti TS	28.83	11.21	29.14	11.52
reactants(s) → trans-anti TS	28.34	10.40	28.76	10.82
cis-gauche TS, loss of H$^+$	468.88	465.80	460.01[c]	456.93[c]
trans-anti TS, loss of H$^+$	441.10	444.86	433.29[c]	437.05[c]

[a] In kcal/mol. [b] $\Delta H = \Delta E + \Delta$ZPE. [c] At 298 K. [d] Experimental gas-phase acidity is 366 ± 2 kcal mol, ref 46.

Results and Discussion

The major focus of this study has been to calculate the transition-state structure of eq 1, as well as the structures of acetaldehyde and its enolate ion, at as high a level as practically feasible commensurate with our resources. Except for a similar study by Saunders,[27] we are not aware of other high-level transition-state calculations for eq 1. On the other hand, numerous *ab initio* calculations, at various levels of theory, have been published for acetaldehyde;[44,45] a high-level (6-311++G**//6-31G*) calculation of the enolate ion also appeared recently.[45]

Table 1 summarizes the energies of various species calculated at the 6-311+G**//6-311+G** and the MP2/6-311+G**//6-311+G** levels. Note that for the aldehyde there are two conformers that differ by less than 1 kcal/mol in energy. In the most stable conformer, aldehyde(e), one of the methyl hydrogens is eclipsed with the carbonyl group, just as reported by Wiberg and Martin.[44] In aldehyde(s), all methyl hydrogens are staggered with respect to the carbonyl group.

In comparing the relative energies for the aldehyde and its enolate ion, we note that our MP2/6-311+G**//6-311+G** calculations yield an acetaldehyde(e) gas-phase acidity of 367.5 kcal/mol (Table 2). This is somewhat lower than Wiberg's value

(40) A value of n different from 2 would result if, e.g., eq 4 is replaced by $\delta_Y = \pi_{bo}(\delta_C + \delta_Y)^u$ and eq 5 is replaced by $\pi_{bo} = \chi(\delta_C + \delta_Y)^v$, with $u \neq 1$, $v \neq 1$, and $n = u + v \neq 2$.

(41) (a) Pross, A.; Shaik, S. S. *J. Am. Chem. Soc.* **1982**, *104*, 1129. (b) Shaik, S. S. *Prog. Phys. Org. Chem.* **1985**, *15*, 197.

(42) Kurz, J. L. *J. Am. Chem. Soc.* **1989**, *111*, 8631.

(43) Gandler, J. R.; Bernasconi, C. F. *J. Am. Chem. Soc.* **1992**, *114*, 631.

(44) Wiberg, K. B.; Martin, E. *J. Am. Chem. Soc.* **1985**, *107*, 5035 and numerous references cited therein.

(45) Wiberg, K. B.; Breneman, C. M.; LePage, T. J. *J. Am. Chem. Soc.* **1990**, *112*, 61.

(46) (a) Lias, S. G.; Bartmess, J. E.; Liebman, J. E.; Leoni, R. D.; Mallard, W. G. *J. Phys. Chem. Ref. Data* **1988**, *17*, Suppl. 1. (b) Bartmess, J. E.; Scott, J. A.; McIver, R. I. *J. Am. Chem. Soc.* **1979**, *101*, 6046.

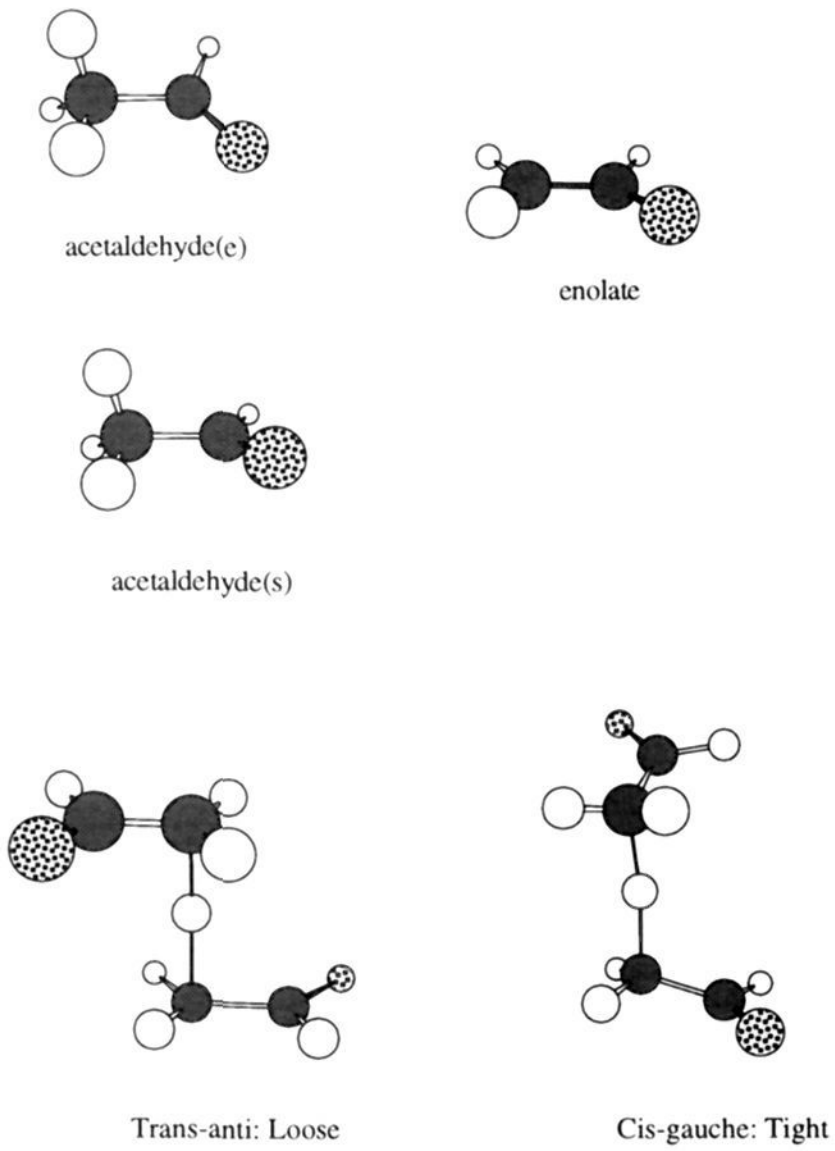

Figure 2. 3D representations of the various structures calculated in this work.

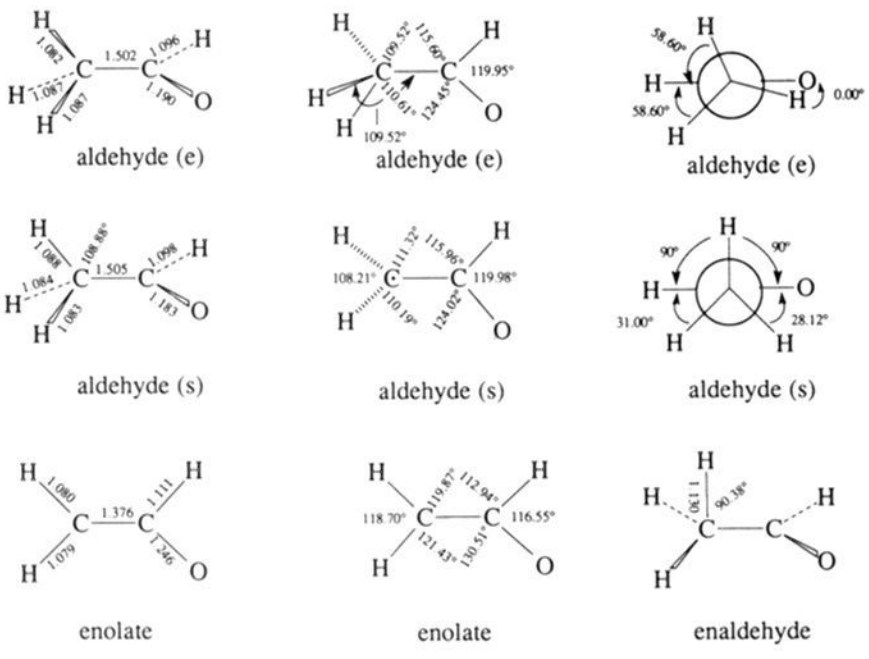

Figure 3. Various schematic views showing the structural parameters of the two aldehyde conformers, the enolate ion, and the enaldehyde.

of 371 kcal/mol[45] and indistinguishable from the experimental gas-phase acidity of 366 ± 2 kcal/mol.[46]

The 3D structures of the two aldehyde conformers and the enolate ion are shown in Figure 2, while the structural parameters calculated at the 6-311+G** level are summarized in Figure 3; they differ only slightly from Wiberg's[45] at the 6-31G* level.

The atomic charges on the two aldehyde conformers and enolate were calculated by four different methods. They are summarized in Table 3. Neither set is directly comparable to Wiberg's charges (available for the enolate), since the latter were obtained using Bader's theory.[47] However, when considering group charges (see below), Wiberg's results, which yield –0.416 for the CH_2 group and –0.584 for the CHO group of the enolate ion, fall within the range of group charges calculated in the present study.

Transition-State Structures: Is There an Imbalance? Our premise in calculating the structure and energy of the transition state with the 6-311+G**//6-311+G** basis set is that the level of theory that has best reproduced the gas-phase acidity of acetaldehyde should also lead to a realistic approximation of the transition state, even though this cannot be proven. In this work we have calculated two transition states which differ in their geometry, charge distribution, and energy. One, designated as cis-gauche TS, is fully optimized and is assumed to represent the "true" transition state of the reaction. It has a nearly tetrahedral α-carbon (Figures 2 and 4) and is very similar to Saunders's cis-gauche TS.[27]

The other, designated as trans-anti, is not a "true" transition state, because it is not a stationary point on the potential energy surface. It has a planar α-carbon (Figures 2 and 4) and is 10.5 kcal/mol higher in energy than the cis-gauche TS (Table 2). This contrasts with Saunders's[27] trans-anti TS, which *is* a stationary point on the energy surface, has a nearly tetrahedral α-carbon, and is of nearly the same energy as the cis-gauche TS.

Our trans-anti TS may be regarded as a model for a more delocalized or less imbalanced transition state. Its calculation was begun by inverting the carbon and oxygen coordinates of the cis-gauche TS and proceeding with partial optimization. However, optimization is incomplete with respect to full coordinate space. The imposed constraint limits the degree of freedom associated with the methylene hydrogens;[48] hence, these hydrogens lie in the plane defined by the carbon and oxygen atoms of the aldehyde fragment. When the constraints are removed, our trans-anti TS collapses into Saunders's[27] trans-anti TS.

The main purpose of discussing this constrained trans-anti TS is that a comparison of its structural parameters with those of the cis-gauche TS will enhance our understanding of the factors responsible for the imbalance (see below).

Due to the symmetry of reaction 1, one may discuss the structural parameters of the two transition states either in relation to the aldehyde as reactant and enolate as product or in relation to the enolate as the reactant and the aldehyde as the product. The former approach will be adopted.

With respect to the question of imbalance, the charge distribution in the transition state relative to that in the aldehyde and enolate ion is the main criterion and will be addressed first. The most meaningful discussion of charges is to consider the CHO and CH_2 groups as single entities and to calculate the charges for these groups by summation of the corresponding atomic charges. These group charges are included in Table 3. For the changes in the group charges that occur upon reaching the transition states or the enolate ion, respectively, we use the symbolism of eq 3 and define δ_C and δ_Y as $(\text{charge})_{TS} - (\text{charge})_{\text{aldehyde}}$ and χ as $(\text{charge})_{\text{enolate}} - (\text{charge})_{\text{aldehyde}}$, respectively. The calculated δ_C, δ_Y, and χ values are summarized in Table 4.

As described in the Introduction, the criterion for an imbalance in the direction of delayed charge delocalization at the transition state is that δ_Y/δ_C should be smaller than $\chi/(1-\chi)$ or that n in

(47) (a) Bader, R. F. W. *Acc. Chem. Res.* **1985**, *9*, 18. (b) Bader, R. F. W. *J. Chem. Phys.* **1986**, *85*, 3133.

(48) Note that the delocalization in the trans-anti TS is a consequence of the planar α-carbon; it is not enforced by constraining the bond lengths in the carbon–oxygen framework, i.e., the constraints imposed on the trans-anti TS are not as stringent as those imposed on the "aldanion" and "enaldehyde" discussed below.

Table 3. Atomic and Group Charges in the Aldehyde, the Enolate Ion, and the Two Transition States (6-311+G**)

	GAUSSIAN 92		GAMESS	
atom	Mulliken SCF[a]	Mulliken MP2[a]	Mulliken SCF[a]	Löwdin[b]
	Aldehyde(e)			
C(CO)	0.290	0.196	0.286	0.080
$C(CH_3)$	−0.487	−0.539	−0.479	−0.242
O	−0.336	−0.236	−0.339	−0.252
H(CHO)	0.095	0.094	0.095	0.086
$H(CH_3$, O-side)	0.159	0.169	0.158	0.109
$H(CH_3$, H-side)	0.140	0.158	0.158	0.109
$H(CH_3$, middle)	0.140	0.158	0.140	0.109
CHO(sum)	0.049	0.055	0.042	−0.086
CH_3(sum)	−0.049	−0.055	−0.042	0.086
	Aldehyde(s)			
C(CO)	0.267	0.178	0.264	0.074
$C(CH_3)$	−0.476	−0.531	−0.469	−0.246
O	−0.328	−0.229	−0.331	−0.247
H(CHO)	0.096	0.095	0.096	0.090
$H(CH_3$, O-side)	0.158	0.170	0.158	0.116
$H(CH_3$, H-side)	0.131	0.148	0.131	0.101
$H(CH_3$, middle)	0.152	0.169	0.151	0.113
CHO(sum)	0.035	0.044	0.029	−0.084
CH_3(sum)	−0.035	−0.044	−0.029	0.084
	Enolate Ion			
C(CO)	0.105	−0.111	0.103	−0.054
$C(CH_2)$	−0.568	−0.451	−0.568	−0.570
O	−0.640	−0.534	−0.636	−0.557
H(CHO)	−0.014	−0.017	−0.014	0.044
$H(CH_2$, O-side)	0.067	0.065	0.066	0.072
$H(CH_2$, H-side)	0.050	0.048	0.049	0.065
CHO(sum)	−0.549	−0.662	−0.547	−0.567
CH_2(sum)	−0.451	−0.338	−0.453	−0.433
	Cis-gauche TS			
C(CO)(1)	0.214	0.053	0.198	0.020
C(CO)(2)	0.212	0.051	0.196	0.019
$C(CH_2)(1)$	−0.656	−0.610	−0.623	−0.441
$C(CH_2(2)$	−0.654	−0.608	−0.621	−0.441
O(1)	−0.475	−0.368	−0.475	−0.405
O(2)	−0.475	−0.368	−0.475	−0.406
H(CHO)(1)	0.035	0.034	0.034	0.067
H(CHO)(2)	0.035	0.034	0.034	0.068
$H(CH_2$, O-side)(1)	0.116	0.128	0.113	0.088
$H(CH_2$, O-side)(2)	0.115	0.128	0.113	0.089
$H(CH_2$, H-side)(1)	0.106	0.120	0.105	0.082
$H(CH_2$, H-side)(2)	0.107	0.120	0.105	0.082
H (transferred)	0.322	0.285	0.297	0.180
CHO(sum)(1)	−0.226	−0.281	−0.244	−0.319
CHO(sum)(2)	−0.229	−0.283	−0.245	−0.319
CH_2(sum)(1)	−0.434	−0.362	−0.405	−0.271
CH_2(sum)(2)	−0.432	−0.360	−0.403	−0.270
	Trans-anti TS			
C(CO)(1)	0.219	0.043	0.210	0.002
C(CO)(2)	0.219	0.043	0.211	0.002
$C(CH_2)(1)$	−0.644	−0.556	−0.616	−0.438
$C(CH_2)(2)$	−0.644	−0.556	−0.618	−0.438
O(1)	−0.520	−0.406	−0.519	−0.432
O(2)	−0.520	−0.406	−0.519	−0.432
H(CHO)(1)	0.042	0.039	0.041	0.069
H(CHO)(2)	0.042	0.039	0.041	0.069
$H(CH_2$, O-side)(1)	0.136	0.140	0.133	0.100
$H(CH_2$, O-side)(2)	0.136	0.140	0.133	0.100
$H(CH_2$, H-side)(1)	0.148	0.146	0.146	0.099
$H(CH_2$, H-side)(2)	0.148	0.146	0.146	0.099
H (transferred)	0.237	0.187	0.212	0.200
CHO(sum)(1)	−0.259	−0.324	−0.268	−0.361
CHO(sum)(2)	−0.259	−0.324	−0.267	−0.361
CH_2(sum)(1)	−0.360	−0.270	−0.337	−0.239
CH_2(sum)(2)	−0.360	−0.270	−0.339	−0.239

[a] See ref 66. [b] See: Löwdin, P. D. *J. Chem. Phys.* **1950**, *18*, 365. Pilar, F. L. *Elementary Quantum Chemistry*; McGraw-Hill: New York, 1990; p 485.

eq 6 should be >1. The δ_Y/δ_C and $\chi/(1-\chi)$ ratios as well as n values[49] included in Table 4 show that, irrespective of the method used to calculate the charges, both transition states suffer from an imbalance, but the imbalance is significantly smaller for the trans-anti TS.

Turning to the C–C and C–O bond lengths, the changes in these bonds upon conversion of the aldehyde into the transition state, Δr^*_{CC} and Δr^*_{CO}, and for the conversion of the aldehyde into the enolate ion, Δr°_{CC} and Δr°_{CO}, respectively, are sum-

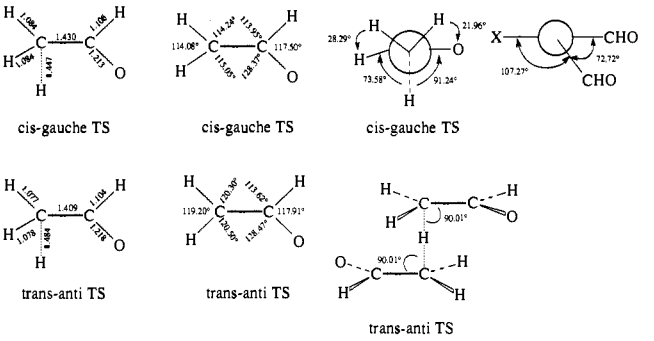

Figure 4. Various schematic views showing the structural parameters of the two transition states. The first three structures of the cis-gauche TS and the first two structures of the trans-anti TS show only one fragment; the structures to the far right represent the entire transition state. For the cis-gauche TS, the Newman projection at the far right is a view along the C···H···C axis; for clarity the hydrogens have been omitted, and a "dummy" atom X has been included to define one of the dihedral angles.

Table 4. Group Charge Differences and Imbalances (6-311+G**)

	GAUSSIAN92		GAMESS	
parameter[a]	Mulliken SCF	Mulliken MP2	Mulliken SCF	Löwdin
	Aldehyde(e) → Enolate Ion			
χ	0.598	0.717	0.598	0.481
$1-\chi$	0.402	0.283	0.402	0.519
$\chi/(1-\chi)$	1.488	2.533	1.488	0.927
	Aldehyde(s) → Enolate Ion			
χ	0.584	0.705	0.576	0.483
$1-\chi$	0.416	0.295	0.424	0.517
$\chi/(1-\chi)$	1.404	2.390	1.358	0.934
	Aldehyde(e) → Cis-gauche TS			
δ_Y[b]	0.277	0.337	0.287	0.233
δ_C[b]	0.384	0.307	0.363	0.357
$\delta_C + \delta_Y$	0.661	0.644	0.650	0.590
δ_Y/δ_C	0.721	1.098	0.791	0.653
n[c]	1.86	1.72	1.70	1.38
	Aldehyde(s) → Cis-gauche TS			
δ_Y[b]	0.262	0.326	0.273	0.235
δ_C[b]	0.398	0.317	0.375	0.354
$\delta_C + \delta_Y$	0.660	0.643	0.648	0.589
δ_Y/δ_C	0.658	1.028	0.728	0.664
n[c]	1.93	1.75	1.72	1.36
	Aldehyde(e) → Trans-anti TS			
δ_Y[b]	0.308	0.379	0.310	0.275
δ_C[b]	0.311	0.215	0.297	0.325
$\delta_C + \delta_Y$	0.619	0.594	0.607	0.600
δ_Y/δ_C	0.990	1.763	1.044	0.846
n[c]	1.38	1.22	1.32	1.10
	Aldehyde(s) → Trans-anti TS			
δ_Y[b]	0.294	0.367	0.296	0.277
δ_C[b]	0.325	0.226	0.309	0.323
$\delta_C + \delta_Y$	0.619	0.593	0.605	0.600
δ_Y/δ_C	0.905	1.624	0.958	0.858
n[c]	1.43	1.25	1.32	1.09

[a] The definition of the parameters is as follows: χ = | (charge on CHO)$_{enolate}$ − (charge on CHO)$_{ald}$|, δ_Y = | (charge on CHO)$_{TS}$ − (charge on CHO)$_{ald}$|; δ_C = | (charge on CH_2)$_{TS}$ − (charge on CHO)$_{ald}$|. [b] Average in cases where the group charges on the two halves of the transition state are different. [c] n calculated as in ref 49.

(49) n is calculated by solving eq 6, which yields $n = \log(\delta_Y/\chi)/\log(\delta_C + \delta_Y)$.

Table 5. C–C and C–O Bond Lengths in the Aldehyde, the Enolate Ion, and the Transition States[a]

	aldehyde(e)	aldehyde(s)	enolate ion	cis-gauche TS	trans-anti TS
r_{CC}	1.502	1.505	1.376	1.430	1.409
r_{CO}	1.190	1.183	1.246	1.213	1.218
Δr°_{CC}[b](e)			−0.126		
Δr°_{CC}[b](s)			−0.129		
$\Delta r^{\ddagger}_{CC}$[c](e)				−0.072	−0.093
$\Delta r^{\ddagger}_{CC}$[c](s)				−0.075	−0.096
Δr°_{CO}[b](e)			0.056		
Δr°_{CO}[b](s)			0.063		
$\Delta r^{\ddagger}_{CO}$[c](e)				0.023	0.028
$\Delta r^{\ddagger}_{CO}$[c](s)				0.030	0.035
$\Delta r^{\ddagger}_{CC}/\Delta r^{\circ}_{CC}$ (e)[d]				0.571	0.738
$\Delta r^{\ddagger}_{CC}/\Delta r^{\circ}_{CC}$ (s)				0.581	0.744
$\Delta r^{\ddagger}_{CO}/\Delta r^{\circ}_{CO}$ (e)				0.411	0.500
$\Delta r^{\ddagger}_{CO}/\Delta r^{\circ}_{CO}$ (s)				0.476	0.556

[a] In angstroms. [b] Δr° = r(enolate) − r(aldehyde). [c] $\Delta r^{\ddagger}$ = r(TS) − r(aldehyde).

marized in Table 5. Included in the table are the fractional bond changes that have occurred upon reaching the respective transition states. Starting with aldehyde(e), for the cis-gauche TS they are $\Delta r^{\ddagger}_{CC}/\Delta r^{\circ}_{CC} = 0.571$ and $\Delta r^{\ddagger}_{CO}/\Delta r^{\circ}_{CO} = 0.411$, while for the trans-anti TS, we have $\Delta r^{\ddagger}_{CC}/\Delta r^{\circ}_{CC} = 0.738$ and $\Delta r^{\ddagger}_{CO}/\Delta r^{\circ}_{CO} = 0.500$. Without putting too much emphasis on the precise numbers, the above ratios indicate that in the trans-anti TS both the shortening of the C–C bond and the lengthening of the C–O bond have made more progress than in the cis-gauche TS. This implies more resonance development and more charge delocalization into the CHO group of the trans-anti TS, in agreement with the conclusion reached on the basis of the charge distributions.

Regarding the $\Delta r^{\ddagger}_{CC}/\Delta r^{\circ}_{CC}$ values, it is interesting that for the cis-gauche TS this ratio (~0.57) is close to the amount of negative charge buildup, i.e., $\delta_C + \delta_Y$ (≈0.63 average). This is the result one would expect on the basis of the model described in the Introduction, according to which the C–Y π-bond order is given by $\chi(\delta_C + \delta_Y)$. On the other hand, for the trans-anti TS, $\Delta r^{\ddagger}_{CC}/\Delta r^{\circ}_{CC}$ (~0.74) is significantly higher than $\delta_C + \delta_Y$ (≈0.60 average), suggesting that π-bond formation is somewhat ahead of proton transfer.

The conclusions derived from the bond lengths are supported by considering the geometry around the α-carbon. For the cis-gauche TS, this geometry suggests that the carbon has retained a significant amount of sp^3 character. This contrasts with the planar α-carbon in the trans-anti TS, which is consistent with the higher π-bond order of the C–C bond.

To summarize, both transition states are characterized by a charge imbalance in the sense that charge delocalization lags behind proton transfer, but this imbalance is significantly greater for the cis-gauche TS. With respect to geometry, the cis-gauche TS appears to be essentially balanced, i.e., the fractional C–C π-bond formation is roughly equal to the amount of negative charge buildup; on the other hand, for the trans-anti TS, the geometric parameters suggest a structural imbalance in the sense that C–C π-bond formation is somewhat ahead of charge buildup.

It needs to be stressed that the conclusion that the charge and structural imbalances of a given transition state are different from each other is not contradictory, because there is no requirement that they should be the same or that the presence of a charge imbalance automatically implies the presence of a structural imbalance. Quite to the contrary, the two imbalances *cannot* be the same, since δ_Y depends on a higher power of $\delta_C + \delta_Y$ (see eq 4) than the π-bond order (see eq 5 and ref 40). This means that even if charge delocalization lags behind charge buildup or proton transfer ($n > 1$), there can easily be a geometric imbalance in the direction of π-bond formation being ahead of proton transfer ($v < 1$, see ref 40). However, according to eq 4, one would expect stronger charge delocalization in the incipient enolate ion for a transition state in which π-bond formation has made greater progress. Our finding that charge delocalization in the trans-anti TS is farther along than in the cis-gauche TS is consistent with this expectation.

Turning to the relative energies of the two transition states, the cis-gauche TS is seen to be more stable than the trans-anti TS by 10.5 kcal/mol (MP2/6-311+G**), despite the stronger resonance development in the trans-anti TS. The lower energy of the cis-gauche TS may be attributed to a greater electrostatic and hydrogen-bonding stabilization, due to the larger positive charge on the transferred proton and the larger negative charge on the CH_2 groups. This is an important conclusion, which is consistent with Gronert's[28] findings of an inverse correlation between transition-state energy and charge on the transferred proton in identity proton transfers of nonmetal hydrides. Another manifestation of the stabilization provided by the electrostatic and hydrogen-bonding effects of the transferred proton is the lower acidity of the cis-gauche TS compared to the trans-anti TS: the removal of the proton from the cis-gauche TS requires 19.9 kcal/mol more energy than proton removal from the trans-anti TS (MP2/6-311+G**, Table 2).

The greater tightness of the cis-gauche TS seen in the shorter C···H···C distance (2 × 1.447 Å for cis-gauche, 2 × 1.484 Å for trans-anti, see Figure 4) is likely to play a stabilizing role as well, although this effect may be a consequence of the larger charges rather than an independent factor. What is notable is that the stabilization provided by the electrostatic/hydrogen-bonding effect is apparently strong enough to more than offset the loss of resonance resulting from the reduced charge delocalization in the cis-gauche TS. This suggests that the electrostatic/hydrogen-bonding stabilization is a major factor that contributes to the imbalance in eq 1. Whether the same is true for reactions in solution is difficult to say, although there is evidence demonstrating the importance of hydrogen bonding in the transition state of proton transfers from certain carbon acids to normal bases in aqueous solution.[50]

More O'Ferrall–Jencks Diagrams. It is instructive to represent eq 1 in terms of a More O'Ferrall[32]–Jencks[29,33] diagram, with separate axes for proton transfer and charge shift. In contrast to the situation in eq 2 or the generalized reaction 3, the base in eq 1 is a charge-delocalized species with its own imbalance at the transition state. This is most conveniently taken into account by constructing a *hexagonal* More O'Ferrall–Jencks diagram, as shown in Figure 5. Corners 1 and 4 are the reactants and products, respectively; corners 2 and 3 are hypothetical states in which the reactant enolate ion (corner 2) or the product enolate ion (corner 3) has its negative charge localized on the carbon ("aldanion"). Corners 5 and 6 are hypothetical states which, just as the top left corner in Figure 1, are somewhat ill-defined but may perhaps be represented by the enolate ion plus a polarized aldehyde, **2**, in which the π-electrons are shifted toward the oxygen; structure **2** may be viewed as a canonical resonance form of this species which we call "enaldehyde."

$$H^+CH_2{=}CH{-}O^-$$
2

It needs to be stressed that the diagram is meant only to qualitatively illustrate the main features of the reaction as they relate to the transition-state structures and the relative timing of proton transfer versus charge shift along the reaction coordinate. Hence, for simplicity, the ion–dipole complexes, which are an important feature in gas-phase reactions[11-19] and will be discussed in detail in a forthcoming paper,[51] have not been included, i.e., all species shown in the corners of the diagram are assumed to be unassociated with their partners. For the same reasons, a discussion of the reaction barriers is being deferred.[51]

(50) (a) Bednar, R. A.; Jencks, W. P. *J. Am. Chem. Soc.* **1985**, *107*, 7117. (b) Bernasconi, C. F.; Wiersema, D.; Stronach, M. W. *J. Org. Chem.* **1993**, *58*, 217.

(51) Bernasconi, C. F.; Wenzel, P. J., manuscript in preparation.

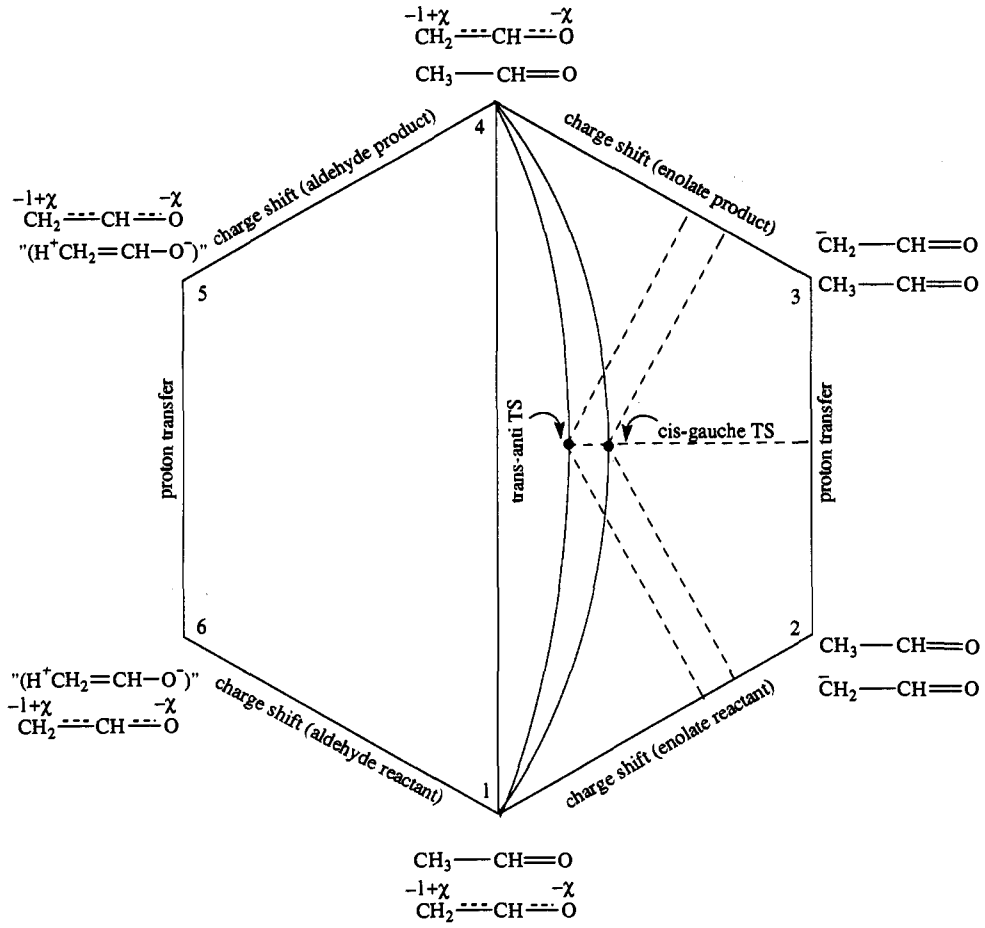

Figure 5. More O'Ferrall–Jencks diagram with separate axes for proton transfer and charge shifts, illustrating the imbalance between proton transfer and charge shift in reaction 1.

Our calculations place a lower limit of 13 kcal/mol on the enthalpy difference between corners 2 and 3 relative to 1 and 4 (Table 2); this corresponds to the energy difference between the planar resonance-stabilized enolate ion and the carbanion constrained to the acetaldehyde geometry ("aldanion," see Figure 2). Corners 5 and 6 are elevated by 25.4 kcal/mol, based on the energy difference between acetaldehyde(e) and the "enaldehyde." The structure of the "enaldehyde" was calculated by freezing the atomic coordinates at the optimized energy of the enolate ion and relaxing the hydrogen coordinates. The resulting structure (Figure 2) yielded no negative eigenvalues in the force field calculation and is therefore not a transition state. That the perpendicular C–H bond of the α-carbon (Figure 3) is still intact is seen from the fact that the enthalpy difference of 25.4 kcal/mol relative to the aldehyde represents only a small fraction of the gas-phase acidity enthalpy (366 ± 2 kcal/mol).[46] However, it amounts to a larger destabilization than that of the enolate ion undergoing the loss of resonance imposed by the geometric distortion into the "aldanion" (13 kcal/mol).[52]

Figure 5 defines three hypothetical limiting pathways of interest. In the first, represented by the vertical line connecting corners 1 and 4, proton transfer and charge shifts are not only concerted but also synchronous; its transition state is in the center of the diagram, where proton transfer as well as charge reorganization both in the enolate reactant and in the enolate product have made 50% progress. The second is a stepwise pathway via corners 2 and 3. It starts with charge localization on the α-carbon in the reactant enolate ion; it is followed by the proton transfer and finally by delocalization of the charge in the product enolate ion. The third is a stepwise reaction via corners 6 and 5; here it is charge shift in the *aldehyde* which precedes and follows the proton-transfer step.

In the *actual* pathways, proton transfer and reorganization are concerted but not synchronous. A precise location of the transition states cannot be given since the energy surface is not known. However, it is evident that the calculated structures require placement *inside the right half of the diagram*, with the more imbalanced cis-gauche TS to the right of the trans-anti TS. Due to the symmetry of the reaction, the two transition states must also be equidistant from corners 1 and 4. The imbalances are clearly recognized by projecting the reaction coordinates onto the enolate charge-shift and proton-transfer axes. We further note that the location of the two transition states inside the right half of the diagram, as well as their relative position, are consistent with a downward tilt of the right side of the energy surface relative to its left side. Such a tilt is suggested by the higher energy of corners 5 and 6 compared to corners 2 and 3.

With respect to potential imbalances in the progress of proton transfer versus π-bond cleavage/formation, they cannot be illustrated by means of Figure 5 because charge shifts and changes in π-bond order are not linearly related to each other. However, they may be represented on the More O'Ferrall–Jencks diagram shown in Figure 6, where the charge-shift axes have been substituted by axes measuring changes in π-bond order. On this diagram, the cis-gauche TS lies on or near the vertical line connecting corners 1 and 4, while the trans-anti TS is located in the left half of the diagram.

It should be noted that, just as for the charge imbalances illustrated in Figure 5, the structural imbalance for the trans-

(52) The "enaldehyde" structure represents the extreme of resonance reorganization being ahead of proton transfer. In contrast, the "aldanion" is the result of proton transfer in the absence of resonance development. As we are unable to manipulate the individual electronic states, we are unable to calculate the electronic states which mix to yield a valence bond configuration mixing model as proposed by Shaik and Pross.[41]

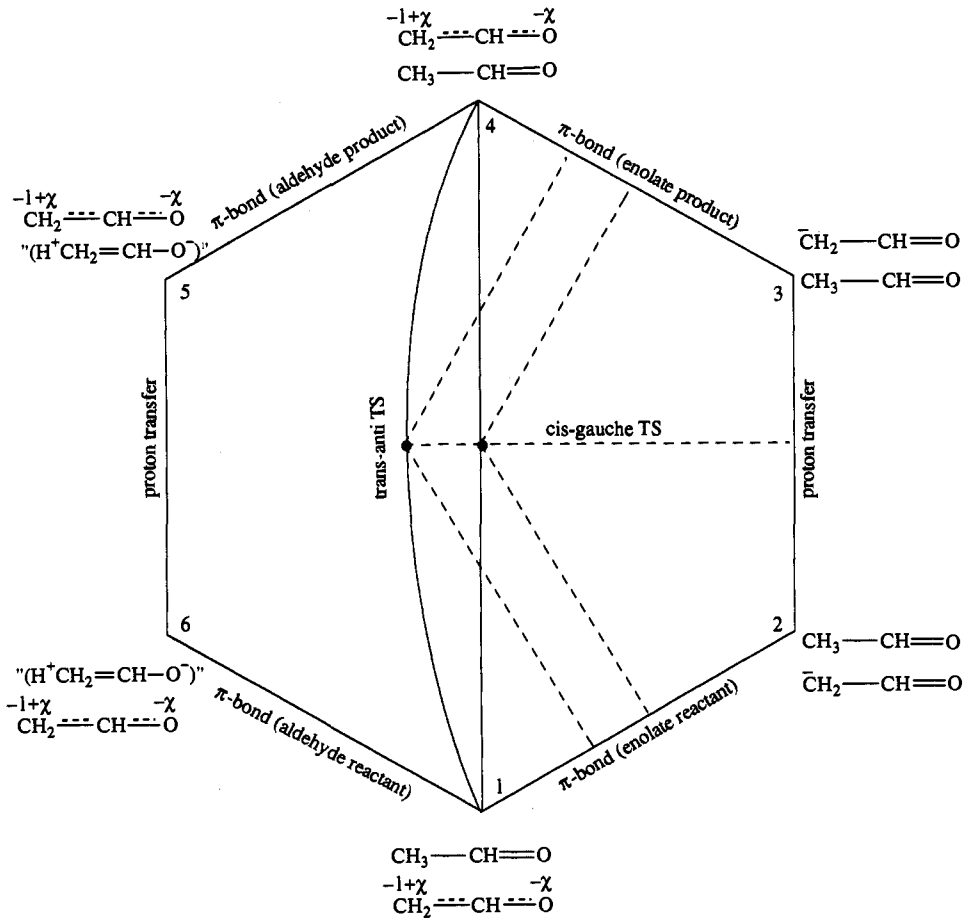

Figure 6. More O'Ferrall–Jencks diagram with separate axes for proton transfer with C–C π-bond order, illustrating balance (cis-gauche TS) and imbalance (trans-anti TS), respectively, between proton transfer and π-bond order in reaction 1.

anti TS illustrated in Figure 6 is represented from the vantage point of the enolate ions (projection of the reaction coordinate onto axes of the right half of the diagram), i.e., the imbalance is seen as arising from the fact that π-bond formation in the incipient product enolate ion is ahead of proton transfer (or that the decrease in π-bond order in the reactant enolate ion lags behind proton transfer). An equally valid view is to see the imbalance from the vantage point of the aldehyde, according to which π-bond development in the reacting aldehyde is ahead of proton transfer (or loss of π-bond character in the incipient product aldehyde lags behind proton transfer).

Comparisons with Solution Reactions. Reaction 1 has not been studied in solution, but imbalances for the deprotonation of nitroalkanes, malononitrile, acetylacetone, and other activated carbon acids by amines in water and Me_2SO–water mixtures have been estimated. These estimates are admittedly crude but, nevertheless, give consistent n values between 2 and 3, with the majority being close to 3.[10] This contrasts with an n value < 2 for the cis-gauche TS of reaction 1. Because the gas-phase n value also suffers from a considerable uncertainty and the solution reactions are not the same as the reaction studied in the gas phase, one needs to exercise caution in drawing conclusions from the comparison of the n values. Nevertheless, one may ask whether it is reasonable that n should be larger in solution than in the gas phase.

There exists substantial evidence that solvation of negative charge on incipient oxyanions typically lags behind the development of the charge.[53] This appears to be the case whether the development of the charge is synchronous with bond changes (e.g., formation of nondelocalized oxyanions)[54–58] or whether charge development itself lags behind bond changes (e.g., formation of a charge-delocalized anion such as a nitronate ion or enolate ion[10,42,43]). This lag in the solvation enhances the charge imbalance in the transition state of proton transfers from carbonyl- and nitro-activated carbon acids. This is reflected in larger intrinsic barriers (or lower intrinsic rate constants) for these reactions in strongly solvating solvents (e.g., water) compared to weakly solvating solvents (e.g., DMSO),[10,43,59,60] as well as in a larger Brønsted α_{CH} value in water compared to DMSO and acetonitrile.[61] Since a larger imbalance implies a higher n value, it is therefore reasonable that n should be larger in solution than in the gas phase.

In terms of eq 6, the increase in n for a solution reaction may be understood as follows. We write eq 7 for the gas phase and eq 8 for solutions.

(53) Or, desolvation of oxyanions is ahead of charge annihilation.

(54) Kresge, A. J. *Chem. Soc. Rev.* **1973**, *2*, 475.
(55) (a) Hupe, D. J.; Jencks, W. P. *J. Am. Chem. Soc.* **1977**, *99*, 451. (b) Hupe, D. J.; Wu, D. *J. Am. Chem. Soc.* **1977**, *99*, 7653. (c) Pohl, E. R.; Wu, D.; Hupe, D. J. *J. Am. Chem. Soc.* **1980**, *102*, 2759.
(56) Jencks, W. P.; Brant, S. R.; Gandler, J. R.; Fendrich, G.; Nakamura, C. *J. Am. Chem. Soc.* **1982**, *104*, 7045.
(57) Terrier, F.; Degorre, F.; Kiffer, D.; Laloi, M. *Bull. Soc. Chim. Fr.* **1988**, 415.
(58) Huskey, W. P.; Schowen, R. L. *Gazz. Chim. Ital.* **1987**, *117*, 409.
(59) Bernasconi, C. F.; Kliner, D. A. V.; Mullin, A. S.; Ni, J. X. *J. Org. Chem.* **1988**, *53*, 3342.
(60) (a) Bernasconi, C. F.; Bunnell, R. D. *Isr. J. Chem.* **1985**, *26*, 420. (b) Bernasconi, C. F.; Paschalis, P. *J. Am. Chem. Soc.* **1986**, *108*, 2969.
(61) α_{CH} = 1.29 and 1.54 for the deprotonation of $ArCH_2NO_2$ in water by morpholine and OH^-, respectively;[30] α_{CH} = 0.92 for the deprotonation of $ArCH_2NO_2$ by $PhCOO^-$ in DMSO;[62] α_{CH} = 0.79 for the deprotonation of $ArCH_2NO_2$ by $PhCOO^-$ in CH_3CN.[43]
(62) Keeffe, J. R.; Morey, J.; Palmer, C. A.; Lee, J. C. *J. Am. Chem. Soc.* **1979**, *101*, 1295.

$$(\delta_Y)_g = \chi_g(\delta_C + \delta_Y)_g^{n_g} \quad (7)$$

$$(\delta_Y)_s = \chi_s(\delta_C + \delta_Y)_s^{n_s} \quad (8)$$

For the case where $(\delta_C + \delta_Y)_s = (\delta_C + \delta_Y)_g = \delta_C + \delta_Y$, the difference in the n values, $n_s - n_g$, is given by

$$n_s - n_g = \frac{\log[(\delta_Y)_s/(\delta_Y)_g] - \log[\chi_s/\chi_g]}{\log(\delta_C + \delta_Y)} \quad (9)$$

The solvation of Y in the product ion enhances charge delocalization and renders χ_s significantly larger than χ_g, but, because solvation of Y is poorly developed at the transition state, $(\delta_Y)_s$ is only minimally enhanced over $(\delta_Y)_g$. Hence the $\chi_s/\chi_g > (\delta_Y)_s/(\delta_Y)_g$, which leads to $n_s > n_g$, i.e., the imbalance should indeed be larger in solution compared to the gas phase.

Conclusions. The "true" transition state (cis-gauche TS) of reaction 1 in the gas phase shows a substantial charge imbalance in the direction of charge delocalization lagging behind proton transfer. Such an imbalance is expected on the basis of Kresge's qualitative model and its translation into eq 6 ($n > 1$). As is evident from a comparison with the less imbalanced and less stable constrained trans-anti TS, the tightness and large positive charge on the transferred proton contribute to this imbalance. Apparently, the loss in resonance stabilization arising from the greater lag in charge delocalization in the cis-gauche TS is more than offset by the tightness and electrostatic stabilization. Such electrostatic stabilization of the transition state has also been found in identity proton transfers of nonmetal hydrides.[28] A similar correlation betweeen tightness and energy of the transition state is known to exist for S_N2 reactions.[63]

Our calculations further suggest that the imbalance in the gas phase may be smaller (lower n in eq 6) than that in solution. This result is not unexpected, because solvation of incipient charges in known to lag behind charge creation or charge transfer, which has the effect of enhancing the overall imbalance.

Methods

Optimizations, force field calculations, and Moeller–Plesset[64] calculations were all carried out using the GAUSSIAN 90[65] or GAUSSIAN 92[66] suites of programs. Standard basis sets (6-311) were used with diffuse (+) and polarization (d on second row elements, p on hydrogen atoms) functions described by Pople.[67] Visualization of the force fields was performed with the GAMESS[68] program using the MOLPLT routine. Optimization of acetaldehyde and its enolate ion at the 6-311+G** level with MP2 correlation at fixed geometry gave the gas-phase acidity. The calculations of the transition-state structures and the distorted aldehyde and enolate were also performed at the 6-311+G** level with MP2 correlation at fixed geometry. The Z-matrices for all calculated species are reported in Tables S1–S7 of the supplementary material.[69]

Assignment of vibrational modes was made according to the method of Wiberg[70] using the experimental data of Hollenstein and Gunthard.[71] A plot of observed frequencies versus calculated frequencies gave a slope of 0.905 (Figure S1).[69] This scaling factor was applied to the force field of all structures calculated at the 6-311+G** level. C_v and zero-point corrections are reported for the scaled vibrations throughout (Tables S8–S14).[69]

Cis-gauche TS. A Z-matrix was constructed such that symmetry through the transferred proton would be enforced. Variables assigned to each bond length, angle, and dihedral angle were identical for each side of the transferred proton. A dummy atom had to be placed near the transferred proton to allow for the definition of a linear relationship between the transferred proton and the methylene carbons of the aldehyde fragments. All dihedral angles were assigned variables which allowed free rotation about the transferred proton. Thus, no center of inversion was enforced for the structure. Optimization was performed at 6-311+G**.

Trans-anti TS. The variables defined for the Z-matrix of the cis-gauche TS led to the restriction that the dihedral angle between the transferred proton and the oxygen of the carbonyl (with the two carbons included in this dihedral) be identical for both of the aldehyde fragments. With free rotation allowed for acetaldehyde, the two fragments need not have the same orientation of transferred hydrogen with respect to the carbonyl oxygen. By defining the dihedral angle with opposite sign for each fragment, the result is to allow a different absolute configuration with respect to the carbonyls in the transition state. The calculated transition state led to a planar methylene carbon atom. The force field then calculated gave a single negative eigenvalue (at 6-311+G**). Note that when the above constraints are removed, our trans-anti TS collapses into the trans-anti TS reported by Saunders.[27]

Aldanion and Enaldehyde. The "aldanion" refers to a structure which has the optimized geometry of the aldehyde(s) for which that hydrogen perpendicular to the aldehyde group is replaced by a dummy atom. This structure was not optimized and represents our attempt at defining an enolate structure for which resonance is disrupted. The "enaldehyde" is a structure in which the enolate geometry is enforced, a proton added, and the geometry of that proton optimized at the 6-311+G** level.

Both the "enaldehyde" and the "aldanion" represent hypothetical structures whose vibrational modes are open to interpretation. None of these modes proved imaginary, though. Hence, we are confident that these structures represent critical points (in the mathematical sense) on the hypersurfaces of both the aldehyde and its enolate. Their use as reference points of the More O'Ferrall–Jencks diagrams is thus justified.

Acknowledgment. This work has been supported by Grants Nos. CHE-8921739 and CHE-9307659 from the National Science Foundation. Additional support was provided by NSF grants through the San Diego Supercomputing Center CRAY YMP/832, account numbers CSC202 and CSC651, and through the Pittsburgh Computing Center on the Cray YMP/832, Grant No. CHE920015P. We are also indebted to Professor Scott Gronert for critical discussions, to Doug Fox of Gaussian Inc. for his helpful suggestions, to Michael Schmidt for his help in providing the GAMESS program, and to Professor William H. Saunders, Jr., for providing us with unpublished results.

Supplementary Material Available: Tables S1–S14 (Z-matrices and vibrational mode analysis) and Figure S1 (scaling force fields in acetaldehyde) (15 pages). This material is contained in many libraries on microfiche, immediately follows this article in the microfilm version of the journal, and can be ordered from the ACS; see any current masthead page for ordering information.

(63) (a) Shaik, S. S. Schlegel, H. B.; Wolfe, S. *J. Chem. Soc., Chem. Commun.* **1988**, 1322. (b) Shaik, S. S.; Schlegel, H. B.; Wolfe, S. *Theoretical Aspects of Physical Organic Chemistry: The S_N2 Mechanism*; Wiley: New York, 1992.

(64) Moeller, C.; Plesset, M. S. *Phys. Rev.* **1934**, *46*, 618. (b) Krishnan, R.; Pople, J. A. *Int. J. Quantum Chem.* **1978**, *14*, 91. (c) Krishnan, R.; Frisch, M. J.; Pople, J. A. *J. Chem. Phys.* **1980**, *72*, 4244. (d) Frisch, M. J.; Head-Gordon, M.; Pople, J. A. *Chem. Phys. Lett.* **1990**, *166*, 281.

(65) Frisch, M. J.; Head-Gordon, M.; Trucks, G. W.; Foresman, J. B.; Schlegel, H. B.; Raghavachari, K.; Robb, M.; Binkley, J. S.; Gonzales, C.; DeFrees, D. J.; Fox, D. J.; Whiteside, R. A.; Seeger, R.; Melius, C. F.; Baker, J.; Martin, R. L.; Kahn, L. R.; Stewart, J. J. P.; Topiol, S.; Pople, J. A. *GAUSSIAN 90*, Revision F; Gaussian, Inc.: Pittsburgh, PA, 1990.

(66) Frisch, M. J.; Trucks, G. W.; Head-Gordon, M.; Gill, P. M. W.; Wong, M. W.; Foresman, J. B.; Johnson, B. G.; Schlegel, H. B.; Robb, M. A.; Replogle, E. S.; Gomperts, R.; Andres, J. L.; Raghavachari, K.; Binkley, J. S.; Gonzalez, C.; Martin, R. L.; Fox, D. J.; DeFrees, D. J.; Baker, J.; Stewart, J. J. P.; Pople, J. A. *GAUSSIAN 92*, Revision B; Gaussian, Inc.: Pittsburgh, PA, 1992.

(67) Hehre, W. J.; Radom, L.; Schleyer, P. v. R.; Pople, J. A. *Ab Initio Molecular Orbital Theory*; Wiley-Interscience: New York, 1986.

(68) Schmidt, M. W.; Baldridge, K. K.; Boatz, J. A.; Elbert, S. T.; Gordon, M. S.; Jensen, J. H.; Koseki, S.; Matsunaga, N.; Nguyen, K. A.; Su, S. J.; Windus, T. L. (together with Dupuis, M.; Montgomery, J. A.) *GAMESS* CRAY (UNICOS) Version; Iowa State University: Ames, IA, 1993.

(69) See paragraph concerning supplementary material at the end of this paper.

(70) Wiberg, K. B.; Walters, V.; Colson, S. D. *J. Am. Chem. Soc.* **1984**, *88*, 4723.

(71) (a) Hollenstein, H.; Gunthard, H. Hs. *Spectrochim. Acta* **1971**, *27A*, 2027. (b) Hollenstein, H. *Mol. Phys.* **1980**, *39*, 1013.